

## Protein–Ion Binding Process on Finite Macromolecular Concentration. A Poisson–Boltzmann and Monte Carlo Study

Sidney Jurado de Carvalho,<sup>†</sup> Márcia O. Fenley,<sup>‡</sup> and Fernando Luís Barroso da Silva<sup>\*,§</sup>

Department of Physics, IBILCE/Unesp, 15054-000 - Rua Cristovão Colombo, 2265, Jd. Nazareth, São José do Rio Preto – SP, Brazil, Department of Physics and Institute of Molecular Biophysics, Florida State University, Tallahassee, Florida 32306, and Department of Physics and Chemistry, Faculdade de Ciências Farmacêuticas de Ribeirão Preto (FCFRP) – USP, 14040–903 Avenida do café, s/no., Ribeirão Preto, SP, Brazil

Received: January 26, 2008; Revised Manuscript Received: October 1, 2008

Electrostatic interactions are one of the key driving forces for protein–ligands complexation. Different levels for the theoretical modeling of such processes are available on the literature. Most of the studies on the Molecular Biology field are performed within numerical solutions of the Poisson–Boltzmann Equation and the dielectric continuum models framework. In such dielectric continuum models, there are two pivotal questions: (a) how the protein dielectric medium should be modeled, and (b) what protocol should be used when solving this effective Hamiltonian. By means of Monte Carlo (MC) and Poisson–Boltzmann (PB) calculations, we define the applicability of the PB approach with linear and nonlinear responses for macromolecular electrostatic interactions in electrolyte solution, revealing some physical mechanisms and limitations behind it especially due the raise of both macromolecular charge and concentration out of the strong coupling regime. A discrepancy between PB and MC for binding constant shifts is shown and explained in terms of the manner PB approximates the excess chemical potentials of the ligand, and not as a consequence of the nonlinear thermal treatment and/or explicit ion–ion interactions as it could be argued. Our findings also show that the nonlinear PB predictions with a low dielectric response well reproduce the  $pK$  shifts calculations carried out with an uniform dielectric model. This confirms and completes previous results obtained by both MC and linear PB calculations.

### I. Introduction

The specific and nonspecific interactions between charged ligands and macromolecules are part of a subject that has been recurrently discussed in literature.<sup>1–10</sup> This fact is related to the importance of such theme for a great number of biochemical processes (e.g., the binding of metallic ions that controls a variety of different intracellular processes, the enzyme modulation by drugs, protein–polyelectrolytes complexation, etc.)<sup>5,11–15</sup> In support of these studies there is a constant development of theoretical methods together with experimental work.<sup>6,16–25</sup>

Different levels for the theoretical modeling of the biomolecular systems have been reported ranging from crude<sup>26,27</sup> to more realistic ones.<sup>6,17,20,21,23</sup> The common simplifications can be either at the electrolyte solution description [from explicit to continuum (or implicit) solvent;<sup>28,29</sup> from explicit mobile ions to a mean field description<sup>18,30</sup> or how the protein is modeled (from a simple macroion with smeared-out charges<sup>26,31</sup> to full atomic description).<sup>20,32–34</sup> There are also intermediate approaches such as the well-known dipole–lattice model of Warshel and co-workers<sup>22,35</sup> and mesoscopic protein models.<sup>3,36</sup> In most cases, a static protein structure determined by X-ray crystallography and NMR spectroscopy is used to build up the atomic or mesoscopic description generally neglecting pH-induced changes in the structure and the structural rearrangements after the binding. Together with a wide number of

descriptions, one often faces the need of a criterion in order to choose a particular model depending on the (biological) question to be answered. It is also a requisite to know the intrinsic approximations assumed by such model to determine when it would provide unphysical results, what approximations that might be required when solving it, and the characteristic consequences of them on the final outcomes, accuracy, and predictions.

Theoretical schemes based on the dielectric continuum framework for the solvent [i.e., in the framework of McMillan–Mayer theory where the solvent only enters by an averaging over of its coordinates and momenta]<sup>28</sup> are largely adopted as standard tools for Structural Biology.<sup>6,17–23,27,37,38</sup> An intense debate between alternative methods to solve such effective Hamiltonian (EH) can be seen in the literature.<sup>18,39–42</sup> The core of such discussions may be summarized in two pivotal issues: (a) how the protein dielectric medium should be modeled, and (b) what protocol should be used when solving this EH (a mean field solution [as assumed in the linear and nonlinear Poisson–Boltzmann approaches) versus a molecular simulation (Monte Carlo or Molecular Dynamics)]. In terms of biological systems, the Debye–Hückel (DH) mean field theory [i.e., the linear form of the Poisson–Boltzmann (LPB) equation. For simplicity and convenience throughout this manuscript we will interchange both terms], which forms the statistical mechanical basis for several theoretical models [e.g., the Tanford–Kirkwood (TK) model]<sup>27</sup> was found to be remarkably well in order to describe both salt screening effects (for symmetric 1:1 electrolyte) and the ionic density distributions around weakly charged macromolecules at low protein concentration.<sup>24,42,43</sup> Its simplicity is absolutely appealing. Conversely, the ionic concentration distribution near

\* To whom correspondence should be addressed. Tel.: +55 (16)3602 42 19. Fax: +55 (16)3602 48 80. E-mail: fernando@fcfrp.usp.br.

<sup>†</sup> IBILCE/Unesp.

<sup>‡</sup> Florida State University.

<sup>§</sup> FCFRP – USP.

highly charged macromolecules is underestimated by the DH approach [even outside the strong coupling regime (i.e., when neutralizing counterions are multivalent, the macromolecular surface charge density  $[\sigma_s]$  is large, the dielectric constant of the solvent is lower than liquid water, or the temperature is smaller than room temperature)]<sup>44–46</sup> demanding the use of the nonlinear form of the Poisson–Boltzmann (NLPB) equation for the correct description of the salt screening effects.<sup>47</sup> In a previous study, we have also shown that the linear form of the Poisson–Boltzmann Equation (which corresponds to a mean field treatment in a linear response scheme, i.e., DH level obtained by a Taylor expansion of the Boltzmann factor of the PB equation with a truncation beyond the first-order terms) satisfactorily predicts the ionic screening effects on binding constant shifts at low protein concentration ( $\approx 0.02$  mM), but only for moderately charged macromolecules ( $< -12e$ , where  $e$  is the electron charge) and if the macromolecule and solvent are assigned the same or similar permittivities.<sup>42</sup> Since nonlinear thermal effects and explicit ion–ion interactions (both in terms of the ionic finite size and electrostatic interactions) are ignored by the TK treatment, a disagreement for highly charged proteins was found (see ref 42) and could be attributed to either one of these simplifications or to both. This is an important matter that remained to be elucidated.

Other research groups have contributed to this discussion studying general electrolyte solution systems. The comparison between results obtained through numerical solutions of Poisson–Boltzmann (PB) equation and Monte Carlo (MC) method have revealed disagreements for systems with multivalent mobile ions<sup>47–49</sup> due the increase of ion–ion correlation effects which are not fully described by the PB approach since it invoked a mean field description for the mobile ions. It can be seen from the definition of the electrostatic coupling parameter ( $\Xi = 2\pi z_k^2 l_b^3 \sigma_s$ , where  $z_k$  is the counterion valency, and  $l_b$  is the Bjerrum length, that is, a measurement of the distance at which two elementary charges in a given solvent interact with thermal energy)<sup>44–46</sup> that increasing the valency of the counterions (i.e.,  $z_k$ ) raises  $\Xi$ . As  $\Xi$  departs from the unity ( $\Xi \gg 1$  indicates that counterions are strongly attracted toward the charged macromolecule), different results from the MC and the PB calculations are expected. As a landmark work in this subject, Guldbrand and coauthors have shown that the PB predictions may also give an even qualitatively inaccurate outcome in some particular experimental conditions (presence of divalent counterions).<sup>50</sup> Moreover, at highly electrostatic coupling regimes ( $\Xi \gg 1$ )<sup>44–46</sup> that may resemble macromolecular ones, effects like overcharging and attraction between equally charged colloidal particles cannot be described by usual numerical schemes based on the PB equation (PBE).<sup>51</sup> Therefore, since previous investigations in a biological oriented context just partially tested the mean field treatment of PB for binding constant shifts calculations, a further critical and complete analysis between different theoretical methods (especially the replacement of PB's linear response by the nonlinear solution) is important in order to define their eventual possible limitations for a particular macromolecular charged system and/or experimental condition. This is the general motivation for the present work.

Other experimental results for electrostatically driven processes require the revisitation of this comparison between PB's mean field predictions and “exact” (within the statistical errors) MC simulations principally for highly charged systems. Linse, co-workers, and other authors have shown that all charged species (and not only the ionic strength) do contribute with the

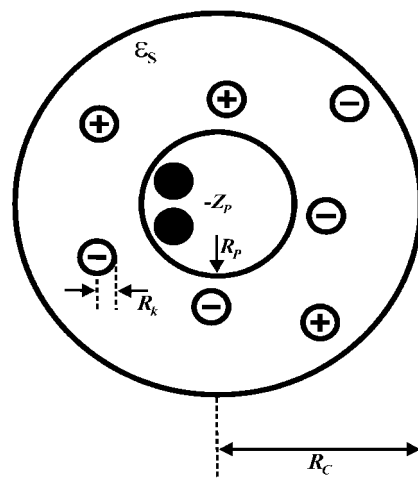


**Figure 1.** Schematic representation of the model system. A charged spherical protein (radius  $R_p$ ) without internal details in a spherical electroneutral cell (radius  $R_c$ ) is seen surrounded by counterions and added salt particles (radii  $R_k$ ). The central protein net charge number is  $Z_p$  (charge  $Q_p = Z_p e$ , where  $e$  is the electron charge). Two binding sites marked with black spheres are also shown inside the left side of the protein.

increase of the Coulomb shielding.<sup>2,25,43,52–54</sup> For instance, outcomes from NMR experiments, MC simulations, and theoretical analysis have demonstrated the decrease of  $\text{Ca}^{2+}$  ions affinity to Calbindin  $\text{D}_{9K}$  and to Calmodulin (more highly charged than Calbindin) due the increase of their (macromolecular) concentrations.<sup>2,25,43,55</sup> This “protein screening phenomena” becomes biologically relevant because the concentration of intracellular proteins *in vivo* can reach an order of magnitude of milimolar<sup>56</sup> and some experimental measurements are performed at high macromolecular concentration [e.g., the typical protein concentration used in NMR experiments is ca. 1 mM].<sup>25,57</sup> Sader and Chan<sup>58</sup> have also shown that mean field theories cannot completely describe the interaction between macroions in confined geometries as an indication that the mobile ion distributions near the macroion are not being satisfactorily determined. Other works have shown similar breakdowns of the PB at high bulk ionic concentrations.<sup>59</sup>

Hence, the purpose of the present work is to define the applicability and accuracy of PB approaches with linear and nonlinear responses for macromolecular electrostatic interactions in solution and to understand the physical mechanisms and limitations behind it. More specifically, we will concentrate on the deviations between exact MC data and PB equation solutions due to the raise of both macromolecular charge and concentration in ligands affinities. Our main contribution will be to clarify the effect of inherent approximations of these two approaches for binding constant shifts.

## II. Thermodynamic Analysis

The binding process of  $n$  ligands to a macromolecule can be quantitatively described through the binding constant  $K$ , whose analysis supplies information about how much this reaction is favored in a set of given experimental conditions. It is by the change in these conditions and the measurements of their effects that one can infer about the physical interactions responsible for the process, the charged ligand–protein association in this case. The variation of binding constants ( $\Delta pK$ ) in relation to the changing on salt concentrations can be written as

$$\Delta[-\log K] = \Delta pK = \frac{1}{kT} \frac{\Delta G^{\text{el}} - \Delta G_{\text{ref}}^{\text{el}}}{\ln(10)} \quad (1)$$

where  $k$  is the Boltzmann constant ( $k = 1.3807 \times 10^{-23} \text{ J} \cdot \text{mol}^{-1} \cdot \text{K}^{-1}$ ),  $T$  is the temperature (in Kelvin), and  $\Delta G^{\text{el}}$  is the electrostatic component of the binding free energy (in kT units) at a given salt concentration ( $C_s$ ). The index *ref* represents a reference state here assumed to be  $C_s = 1 \text{ mM}$ . All other contributions to the total binding free energy ( $\Delta G^{\text{other}}$ ) such as structural changes, short-range interactions, solvation, and so forth are assumed to be either small or virtually invariant with respect to the changes in salt and/or macromolecular concentration ( $\Delta G^{\text{other}} - \Delta G_{\text{ref}}^{\text{other}} \approx 0$ ).<sup>18,42,55,60–62</sup> Even calmodulin (another EF-hand protein that binds four calcium ions) that exhibits significant large structural changes upon  $\text{Ca}^{2+}$  binding can be successfully modeled by such simplified assumption.<sup>43,55</sup>

The binding (electrostatic) free energy  $\Delta G^{\text{el}}$  is given as a function of the electrostatic component of free energy  $G^{\text{el}}$  of the macromolecule in the holo (with the ligands) and apo (without the ligands) forms and the excess chemical potential  $\mu_{\text{F}}^{\text{ex}}$  of the free ligand(s) in solution,

$$\Delta G^{\text{el}} = G_{\text{holo}}^{\text{el}} - G_{\text{apo}}^{\text{el}} - n\mu_{\text{F}}^{\text{ex}} = \mu_{\text{S}}^{\text{ex}} - n\mu_{\text{F}}^{\text{ex}} \quad (2)$$

where  $n$  is the number of ligands and  $\mu_{\text{S}}^{\text{ex}} (= G_{\text{holo}}^{\text{el}} - G_{\text{apo}}^{\text{el}})$  is the isothermic work required for the insertion of these ligands into their corresponding binding sites.

### III. Methods

**Model Systems.** The model used in this work is analogous to the charged spherical one described in details elsewhere [see refs 42 and 43]. The whole system is composed of one single macromolecule modeled as a charged hard-sphere (like a macroion) of radius  $R_p$  and free mobile ions (added salt particles and counterions). All these species are confined within a spherical cell (electrically neutral) of radius  $R_c$  determined by the macromolecular concentration  $C_p$ . The macromolecule without internal details in its apo form is fixed at the center of the simulation cell as shown in Figure 1. The surrounding electrolyte aqueous solution 1:1 is treated at the McMillan–Mayer level as given by the so-called restricted primitive model.<sup>63</sup> Mobile free ions (counterions and added salt) are represented by hard-spheres of radii  $R_k = 2 \text{ Å}$  carrying a central charge  $Q_k = z_k e$ , where  $e$  is the electron charge ( $1.6 \times 10^{-19} \text{ C}$ ) and  $z_k$  is the ionic valency ( $z_k = +1$  for the cations, and  $z_k = -1$  for the anions). The solution static dielectric constant  $\epsilon_s$  and temperature  $T$  are set equal to 78.7 and 298.15 K, respectively.

Although it is perfectly possible and somewhat customary to use the tridimensional structure of specific proteins (e.g., obtained from the Protein Data Bank),<sup>64,65</sup> this crude simplified macromolecular model is necessary in order to keep our analysis as general as possible, and not constrained to a specific biological system. This protocol is often invoked for this purpose.<sup>42,62,66</sup> Conversely, we preserve some biological features by assuming a model that is a “caricature” of Calbindin D<sub>9k</sub> (CaB)<sup>67</sup> [a small globular protein with 722 atoms (46 charged residues for the wild type apo form giving a net charge of  $-8e$  at pH  $\approx 7.5$ ) that binds two calcium ions ( $\text{Ca}^{2+}$ ) with high affinity<sup>68</sup>]. Most proteins have the activity site placed close to its surface as seen in CaB which keeps our present study in a general physical chemistry context.  $R_p$  is set equal to 14 Å with the two  $\text{Ca}^{2+}$  binding sites located at positions (7.314, 7.114,

$-1.607$ ) and (10.503,  $-3.509$ ,  $-0.364$ ). These coordinates are given in Ångströms and were directly taken from the crystallographic data (PDB-ID 3ICB)<sup>64,65</sup> with the assumption that the protein center of mass is at the origin of the Cartesian axis. Ligands are represented like any mobile ions, that is, by a hard sphere of charge  $Q_l = +2e$  (valency  $z_l = +2$ ) and radius  $R_l = 2 \text{ Å}$ . The protein charge  $Q_p = Z_p e$  will be varied from  $-4$  to  $-24e$  (for its apo form) aimed to explore the effect of varying the macromolecular charge. For the protein net charge number  $Z_p = -8$ , the model corresponds to CaB at pH  $\approx 7.5$  and gives similar predictions in comparison with laboratorial measurements.<sup>42</sup>

Any kind of macromolecular polarizability can be introduced in this simple model only considering it as a spherical low dielectric cavity of radius  $R_d$  and dielectric constant  $\epsilon_p$ .<sup>42</sup> The effect of this assumption is to produce a dielectric interface, which subject is rather controversial and has been under intense debate in the literature.<sup>4,30,35,42,62,69–80</sup> Even the physical meaning of a dielectric constant is a problematic issue in this context.<sup>78,81</sup> It is well established that certain electrostatic properties, such as electrostatic free energies and others, computed within the framework of the PBE can be highly dependent on the assumed values of the internal dielectric constant.<sup>69,82,83</sup> Moreover, many times the dielectric constant of the biomolecule is assumed to be an adjustable or empirical parameter (specific for a given model) whose choice is based on obtaining the best agreement between the predicted properties and the experimental results with physically weak arguments.<sup>62,78</sup> As an example of the scattered views on this issue, numbers for  $\epsilon_p$  from 2 to 80, sigmoidal-distance dependent dielectric function and multiple dielectric constants have been employed in the literature.<sup>4,30,35,42,62,69–81,84–86</sup> In general, protein’s interior dielectric constants in the range of 2–8 are more typically used within the biophysical works in a well contrast with the traditional practice in colloid chemistry (where a uniform dielectric permittivity is assigned to the whole system). In the biophysically oriented approach, some authors employ a value of 2 for the macromolecule, when there is no reorientation of fixed dipoles and peptide bonds. Values of 4–6 are used for processes that have some small reorientation of the dipoles.<sup>87</sup> Because there is no consensus in this matter, it is particularly interesting to consider the situation when a uniform dielectric permittivity can be assigned to the whole system. This is in good agreement with the traditional practice in colloid chemistry and avoids the need to handle a not well-defined quantity. Supporting this view in protein electrostatic problems, it has been found that an arbitrarily high value of the protein’s interior dielectric constant provides the best prediction of protein  $pK_a$  shifts.<sup>75,83,88</sup> Mean-field calculations using a low value of  $\epsilon_p$  for the protein’s interior predict calcium binding constant shifts that are qualitatively different from those observed by experiments.<sup>70</sup> On the other hand, the experimental behavior is very well predicted by Monte Carlo simulations and a Tanford–Kirkwood scheme when the dielectric constant of the solvent is used throughout the system ( $\epsilon_p = \epsilon_s$ ).<sup>89</sup> Using a low dielectric response ( $\epsilon_p < \epsilon_s$ ) for the macromolecule can give unphysical results when used to predict mutational effects on calcium binding constants.<sup>42</sup> Conversely, calculations performed with a uniform continuum model successfully reproduced experimental data.<sup>55,70,89</sup> More sensitive electrostatic mechanism responsible for the macromolecular complexation are also well described by the homogeneous dielectric description.<sup>2,3,15,61,90–94</sup> Hence, in an effort to understand how the results reported here are affected by the presence of a dielectric discontinuity we have performed PB calculations



using extreme values of the internal biomolecular dielectric constant: 2 and 78 with  $R_d = R_p$ , where the latter represents conditions close to a uniform dielectric medium. As far as we are aware, this is the first time that such complete comparison is done for ligand (calcium) binding shifts.

Given a symmetrical 1:1 electrolyte in concentration  $C_s$ , the number of cations  $N_+$  and anions  $N_-$  are given by

$$N_+ = V_c N_a C_s + \frac{|Q_p|}{e} \quad (3)$$

$$N_- = V_c N_a C_s \quad (4)$$

where  $N_a$  is the Avogadro number ( $N_a = 6.022 \times 10^{23} \text{ mol}^{-1}$ ) and  $V_c = 4/3\pi R_c^3$  is the cell volume. The additional term in the eq 3 is due the number of added counterions in the system so that the cell preserves the electroneutrality condition ( $Z_p < 0$  in all calculations).

Each two charged sites  $i$  and  $j$  (either the protein central charge, a free mobile ion or the ligand) with a spatial separation distance  $r_{ij} > R_i + R_j$  contributes to the electrostatic potential energy simply by the ordinary Coulomb potential

$$u^{\text{el}}(r_{ij}) = \frac{z_i z_j e^2}{4\pi\epsilon_0 \epsilon_s r_{ij}}, \quad (5)$$

where  $\epsilon_0$ ,  $z_i$ , and  $z_j$  denote the vacuum permittivity ( $\epsilon_0 = 8.854 \times 10^{-12} \text{ C}^2/\text{Nm}^2$ ) and the valency of charges  $i$  and  $j$ , respectively. The Coulomb collapse is avoided by the inclusion of a short-ranged hard core overlap restriction among the charges ( $u^{\text{hs}}$ ) when  $r_{ij} \leq R_i + R_j$

$$u^{\text{hs}}(r_{ij}) = \begin{cases} \infty & , \quad r_{ij} \leq (R_i + R_j) \\ 0 & , \quad \text{otherwise} \end{cases} \quad (6)$$

Equation 6 accounts also for the macromolecular excluded volume ( $R_i = R_p$  when specie  $i$  is the protein).

A one-body external field  $v^{\text{ex}}(r_i)$  is imposed in order to maintain all mobile species inside the simulation cell and to define the macromolecular concentration. This cell boundary constraint acts as a hard wall

$$v^{\text{ex}}(r_i) = \begin{cases} 0 & , \quad (R_i + R_p) \leq r_i \leq R_c \\ \infty & , \quad \text{otherwise} \end{cases} \quad (7)$$

This cell model has the extra benefit that all electrostatic interactions within the cell can be exactly treated in the sense that no cutoff scheme or potential truncation and the corresponding techniques used to remedy them (e.g., Ewald summation,<sup>95</sup> need to be employed.

Consequently, the full configurational energy of the system is defined by the combination of eqs 5–7

$$U(\{\mathbf{r}_k\}) = \sum_{i=1}^{N_c+N_s} v^{\text{ex}}(r_i) + \frac{1}{2} \sum_{i=1}^N \sum_{j=1}^N (u^{\text{el}}(r_{ij}) + u^{\text{hs}}(r_{ij})), \quad (8)$$

where  $N_c$  and  $N_s$  are the number of mobile counterions and added salt ions, respectively. The total number of charges is  $N = N_c + N_s + N_p$ , where for all calculations reported here  $N_p$

was set equal to 1 (for the sake of convenience, a single central charge is used, i.e., the protein may be seen as a charged macroion here).

**Monte Carlo simulations.** The standard Metropolis Monte Carlo (MC) method<sup>96,97</sup> in the canonical ( $NVT$ ) ensemble was used to solve the effective Hamiltonian described above sampling equilibrium configurations. Typically, the equilibration was carried out during  $10^5$  configurations per particle. Mean properties were extracted during more  $10^7$  configurations per particle after the equilibration. Calculations details are well established in literature.<sup>2,24,42,55,89</sup>

Chemical potentials for the ligands were obtained through the modified version of the Widom insertion method conveniently adapted for electrolyte solutions.<sup>98</sup> Alternatively the correction protocol suggested by Sloth and Sørensen<sup>99</sup> could be used together with the standard Widom method.<sup>100</sup> Insertions of the (virtual) ligand particle in random position within the simulation cell during the production run was used to measure the chemical potential for the free ligand ( $\mu^{\text{ex}}$ ). The bound chemical potential ( $\mu^{\text{ex}}$ ) was calculated trying to place the ligand as a perturbation particle at the binding sites positions. All attempts to insert the Widom particles do not interfere in the Markov chain. Numerical fluctuations were estimated from the division of the production phase into 10 blocks. The final mean value of  $\mu^{\text{ex}}$  and  $\mu^{\text{ex}}$ , and their respective standard deviations were given through the values obtained in each simulation block.

Calculations were done at both low ionic strength ( $C_s = 1 \text{ mM}$ ) and around physiological salt concentrations ( $C_s = 100 \text{ mM}$ ), while  $C_p$  was in the range of 0.02 to 2 mM whose choice was done accordingly to ref 43. The value for the smallest  $C_p$  is based on typical experimental conditions.<sup>89,101</sup>

**The Poisson–Boltzmann Approach.** For a given effective Hamiltonian as the one described above (see eq 8) one can invoke a mean field approximation in order to solve this model. An accepted and widespread route is to replace explicit free ions in the model by their mean field behavior (also assuming point particles and normally neglecting their finite size). This is commonly the approach followed in theoretical works based on the Poisson–Boltzmann (PB) and/or the Debye–Hückel theories (i.e., LPB).<sup>17,18,21,23,27,42,47,51,53,102</sup>

The organization of ions around a spherical charged particle or planar surface in electrolyte solutions is a classical problem in physical chemistry and frequently studied using the PB equation, which also forms the basis of several theories in the colloidal domain.<sup>103,104</sup> The PB equation is a particular case of the Poisson equation,<sup>105,106</sup> where the mobile ionic charges densities are supposed to be given by the Boltzmann's distribution. The well-known PB equation for a two component system at a charged surface immersed in a  $z_i:z_j$  symmetrical salt solution of concentration  $C_s$  may be<sup>53,102,107</sup>

$$\nabla^2 \phi = \frac{2z_i e C_s}{\epsilon_0 \epsilon_s} \sinh\left(\frac{z_i e \phi}{kT}\right) \quad (9)$$

where  $\phi$  is the mean electrostatic potential. Nevertheless,  $\phi$  is assumed here to be a result from the average force acting on one particular ion from the interactions of both the charged surface and all the other ions, i.e.,  $\phi$  is taken as equal to the potential of mean force divided by the charge of the ion.<sup>102,108,109</sup> The discrimination between the “mean electrostatic potential” and the “potential of mean force” in this context is presented pedagogically by Lyklema.<sup>110</sup>

Equation 9 is a nonlinear equation and its mathematical solution (analytical or numerical) is quite complex and tricky.

Analytical solutions are possible only for very simple cases. One of these special situations where its analytical solution is known is the infinite charged planar surface case,<sup>108,111,112</sup> which is usually described as the Gouy–Chapman case.<sup>112</sup> For real proteins where the charge distribution is not spherically symmetric (even for globular proteins), an analytical solution is far from trivial. Even proteins with similar sizes may have large differences on their electrostatic profiles [e.g., lysozyme and  $\alpha$ -lactalbumin have almost the same radius of gyration ( $\approx 28$  Å) while their electric dipole moment numbers at pI (isoelectric point) are 24 and 82 (in units of Å), respectively<sup>113</sup>]. In most cases including the applications on biomolecules, numerical techniques are required to solve the linear or nonlinear PBE. Different numerical methods are available, for example, the “finite element (FE) method”,<sup>114–117</sup> “finite difference (FD) method”,<sup>37,114–116,118,119</sup> “boundary element (BE) method”,<sup>88,114–116,120,121</sup> and the hybrid boundary element (HBE) method solver.<sup>23,122</sup> There are also a number of generalized program packages available principally for applications to study the (bio)molecular phenomena.<sup>20,37,118,119,123–126</sup>

Most of the biomolecular applications assume the “infinite macromolecular dilution regime”. A classical example is the Tanford–Kirkwood (TK) model. It is a dielectric continuum model that assumes that the protein may be modelled by a hard-sphere treated as a low dielectric permittivity body immersed in a medium (the electrolyte solution) with high dielectric permittivity. With respect to the rigid macromolecular reference frame with fixed charged groups, the salt ions and other charged ligands are supposed to be in relative motion throughout the infinite solvent medium. The Debye–Hückel potential is used to describe the effective interactions between the charged macromolecule and the mobile ions, i.e., the free ions just “participate” through their mean-field contribution. All protein charges at their specific structural (native) locations are assumed to be inside the low dielectric sphere.<sup>27,42</sup> Finite macromolecular concentrations are simply neglected.

In order to incorporate the finite macromolecular concentration effect, the traditional spherical cell model (as suggested by the TK model) can be used together with the assumption that the mean electric field at the cell boundary  $r = R_c$  is null [ $\phi(R_c) = 0$ ].<sup>105,106</sup> This boundary condition guarantees the cell electroneutrality condition. There are other more realistic alternative methods for simulations that account for macromolecular concentration effects. In a recent work, the classical TK model was improved and became suitable for the description of the effect of protein concentration on ion binding with a simple modification of the definition of the screening length based on works from the colloidal literature: the inclusion of the counterions (responsible for cell electroneutrality) in the Debye screening length.<sup>43,52–54,127</sup> Applying the same reasoning, the nonlinear PB equation may also be written in a more general form from the inclusion of the counterion concentration

$$\nabla^2 \varphi = -\frac{N_a e}{\epsilon_0 \epsilon_s} [C_s \exp(-\beta \varphi) - C_s \exp(\beta \varphi) + \frac{|Q_p|}{e} C_p \exp(-\beta \varphi)] \quad (10)$$

where  $\beta = 1/kT$ . This equation is here designated as the modified NLPB equation (MNLBPB) and is written in a unit-independent format.

For a low-charged ligand (e.g.,  $Mg^{2+}$ ) and the linear mean field response (DH level), the excess chemical potential for the free ligand ( $\mu_F^{\text{ex}}$ ) reads

$$\beta \mu_F^{\text{ex}} = -\frac{\kappa Z_l^2}{8\pi \epsilon_0 \epsilon_s (1 + 2\kappa R_l)} \quad (11)$$

where  $R_l$  is the radius of the ligand, and  $\kappa^{-1}$  is the Debye screening length (we shall also refer to it as  $\kappa_{\text{DH}}^{-1}$ ). This equation was always used to compute  $\mu_F^{\text{ex}}$  in our PB calculations unless stated otherwise. Alternatively,  $\mu_F^{\text{ex}}$  can be obtained by numerical calculations which turned out to be a key point in our present discussion. Nevertheless, the common protocol for PB calculations is to assume the standard  $\kappa$  definition [ $\kappa = [(e^2/\epsilon_0 \epsilon_s kT) \sum_{k=1}^N C_k (z_k)^2]^{1/2}$ , where  $N_k$  is the number of particles of specie  $k'$  (valency  $z_k$ )],<sup>109</sup> and obtain  $\mu_F^{\text{ex}}$  by the analytical formula (eq 11). In this case, linear and nonlinear PB calculations will give virtually the same value for  $\mu_F^{\text{ex}}$ . These outcomes are not appropriated to properly describe the finite macromolecular concentration regime. This can be improved for instance by the replacement of the Debye's  $\kappa$  (i.e.,  $\kappa_{\text{DH}}^{-1}$ ) by Beresford–Smith's  $\kappa$  suggestion ( $\kappa_{\text{BS}}^{-1}$ ).<sup>53,54</sup>

For our purposes, it is necessary to carry out calculations assuming both an infinitesimally small macromolecular concentration and at a finite macromolecular concentration. Therefore, different PB solvers were employed in our calculations. In the infinite macromolecular dilution regime ( $C_p \rightarrow 0$ ), electrostatic components of free energies  $G_{\text{apo}}^{\text{el}}$  and  $G_{\text{holo}}^{\text{el}}$  were obtained with the DelPhi package, version II (which uses the FD method),<sup>6,34</sup> through the difference between the total energy at a particular salt concentration and the total energy at null ionic strength. This procedure is necessary in order to exclude the grid self-energy contribution which has no physical meaning. For each experimental condition, a set of calculations with various numerical parameters were carried out as a manner to evaluate the dependence of them in our outcomes. The grid resolution was changed from 2.0 to 4.0 grids/Å, while the box percentage fill was changed from 20 to 90%. The Debye–Hückel boundary condition was assumed, that is, the potential at the edge of the lattice ( $\phi_{\text{edge}}$ ) used to numerically solve the PB equation was forced to be

$$\varphi_{\text{edge}} = \sum_{i=1}^{N_p} q_i \frac{e^{-r_i/\kappa}}{\epsilon_s r_i} \quad (12)$$

where  $q_i$  and  $r_i$  correspond to the  $i$ -th protein charge and the separation distance between the lattice boundary point and the protein charge  $i$ , respectively. The sum of Debye–Hückel potentials considers all  $N_p$  protein charges.<sup>87</sup>

The dependence of all numerical input parameters on the outcomes was verified. The combination of both the grid resolution and box percentage fill parameters that resulted in more stability (i.e., variations of less than 0.06%) simultaneously for both the salt-free and added-salt cases were chosen. Typical values for ion-exclusion layer (2 Å) around the macromolecule and the solvent probe radius (1.4 Å) were used. All the results for the pK shifts due to varying ionic strengths were also compared with data obtained from calculations carried out with the APBS package (which also uses the FD method).<sup>126</sup> Except for the macromolecular charge number  $Z_p = -4$  where we did find a deviation of 17% (DelPhi resulted in  $\Delta pK = 1.46$  kT, while APBS, 1.76 kT), the deviation was lower than 3% in all other cases.

The hybrid boundary element and finite-difference PBE solver developed by Boschitsch and Fenley was also used.<sup>23,122</sup> In order to obtain the LPB solution using the fast BE method, the

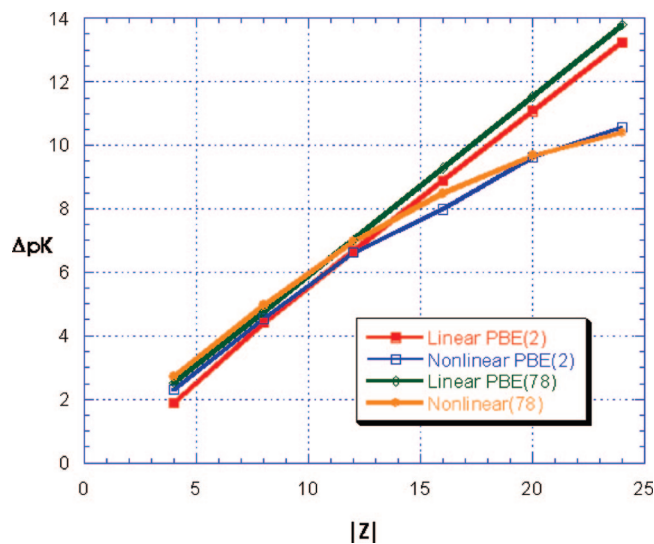


**Figure 2.** Total shift in ion binding constant  $\Delta pK$ , owing to solution ionic strength, is plotted as a function of the protein net charge number ( $Z_p$ ). A reference  $C_s = 1$  mM is chosen, and the final salt concentration is  $C_s = 500$  mM. Results from PB calculations (LPB and NLPB) for different dielectric interfaces ( $\epsilon_p = 2$  and  $\epsilon_p = 78$ ) are compared as indicated in the plot. The solvent dielectric constant ( $\epsilon_s$ ) is 78 in both cases. All calculations were carried out with the hybrid boundary element and finite difference PBE solver assuming an infinite dilution regime.<sup>122,23</sup>  $pK$  shifts (here  $pK_{BEM}$ ) are given in  $kT$  units.

spherical surface is discretized into a collection of 1280 curvilinear triangular elements and the surface solution (electrostatic potential and normal component of the electric field) is obtained with nonlinear contributions omitted. More finely resolved surface grid resolution was found to have a minimal impact on the computed electrostatic free energies. The nonlinear correction is obtained by the finite difference method using a  $65 \times 65 \times 65$  regular three-dimensional (3D) mesh. The total extent of the 3D uniform Cartesian grid was at least four times the sphere diameter in order to produce minimal outer boundary errors. It is assumed that  $\phi = 0$  at the outer boundaries. In most calculations, five multigrid levels were considered to solve the finite difference (FD) equations. We shall refer to resulting data with the subscript  $BEM$ . We assume that there is no ion exclusion region. For details about these PB equation algorithms the reader is referred to elsewhere.<sup>23,122</sup>

The computational program PBCell<sup>125</sup> was used to solve the PB equation for the spherical cell model through the FD method. In this case, the boundary condition at the cell border is  $\nabla\phi(R_c) = 0$ . Different macromolecular concentrations were investigated as done by the MC simulations. This is how we have acquired salt concentration distribution profiles at several  $C_p$ s.

#### IV. Results and Discussion

**The Dielectric Interface.** First, we have examined the charge dependence of  $\Delta pK$  on the net charge of the proteins based on both linear and nonlinear PBE solutions. Our results show that the linear dependence of  $\Delta pK$  as a function of the protein net charge, as depicted in Figure 2 based on a homogeneous dielectric medium ( $\epsilon_p = \epsilon_s = 78$ ), agrees with previous studies<sup>43</sup> and is also captured when the dielectric discontinuity is present ( $\epsilon_p \neq \epsilon_s$ ). In both approaches, a null ionic exclusion region surrounding the biomolecule is adopted in order to enlarge the dielectric interface effects. Moreover, our results based on nonlinear PBE solution show that linear behavior of  $\Delta pK$  as a function of the protein net charge no longer holds, as shown in

Figure 2 for the nonlinear PBE curve. This is observed for both extremes of protein interior dielectric constants ( $\epsilon_p = 2$  and  $\epsilon_p = 78$ ). At low protein net charges the nonlinear and linear PBE results converge (see Figure 2) as expected. These results are obtained independent of the specific PBE parameters employed in the calculations. Therefore, the general trends portrayed in Figure 2 for the linear and nonlinear PBE solutions seem universal and independent of both the exact PBE numerical parameters employed in the calculations and the protein dielectric response.

Next, we look into the salt dependence of  $\Delta pK$ . The ionic dependence of  $pK$  shifts for larger protein net charges is different for the linear and nonlinear PBE solutions but these differences become very small for weakly charged proteins. The increase of  $\Delta pK$  with increasing salt concentrations is more pronounced with the linear PBE as opposed to the nonlinear PBE solution. This is also a general result that does not depend on the specific PBE parameters such as protein dielectric constant, and the presence or absence of ion exclusion region. Over the whole range of salt here considered, the slope of the  $\Delta pK$  versus salt concentration curves are practically independent of the assumed value of the protein dielectric constant. For instance, for the case where the protein net charge is  $-16e$ ,  $\Delta pK$  obtained with the nonlinear PBE solution over a limited moderate salt range is 0.57 and 0.59, when the protein dielectric constant is 2 and 78, respectively. These difference is much smaller than typical experimental errors (ca. 0.3  $pK$  units). For the linear PBE solution the slopes of the  $\Delta pK$  curves versus salt concentration for the two different protein dielectric constants are also similar. On the other hand, the  $\Delta pK$  values are slightly more sensitive to the protein dielectric constant. For the example, for the same case where the protein net charge is  $-16e$ , fixing the NaCl at 50 mM and invoking the nonlinear PBE, we have obtained  $\Delta pK$  equal to 4.9 and 5.1 when the protein dielectric constants are 2 and 78, respectively. However, these differences are still small when considering the typical errors in experimentally determined  $\Delta pK$  values.

In the limit of low salt concentration, the  $\Delta pK$  values are practically independent of the protein's interior dielectric constant, that is, the presence of dielectric discontinuity does not have any effect. These results lend support to an analytical result reported in the literature<sup>122</sup> that states that in the limit of low salt conditions (approaching no added salt) the salt derivative of the electrostatic free energy for a sphere containing a central charge is not dependent on the dielectric ratio between the protein interior and exterior but solely on the solvent dielectric constant and protein net charge. We have shown that the electrostatic solvation free energies of proteins modeled at the all-atom level in low salt conditions follow closely this analytical result, which is independent of the particular choice of the interior protein dielectric constant.<sup>122</sup>

Moreover, we have also shown (Fenley, unpublished data) that the salt dependence of the protein (peptide)–nucleic acid association constant is likewise very weakly dependent on the interior dielectric constant in the range of physiological salt conditions. However, it should be pointed out that based on an analysis of hundreds of protein(peptide)–nucleic acid complexes we observe that the electrostatic contribution to the total binding free energy is very sensitive to the assumed value of the interior dielectric constant (Fenley, unpublished data). The electrostatic binding free energy can become favorable or unfavorable depending on the assumed biomolecular dielectric constant. Moreover, the examination of how the protein's interior dielectric constants affect the salt dependence of  $pK$  values (e.g.,



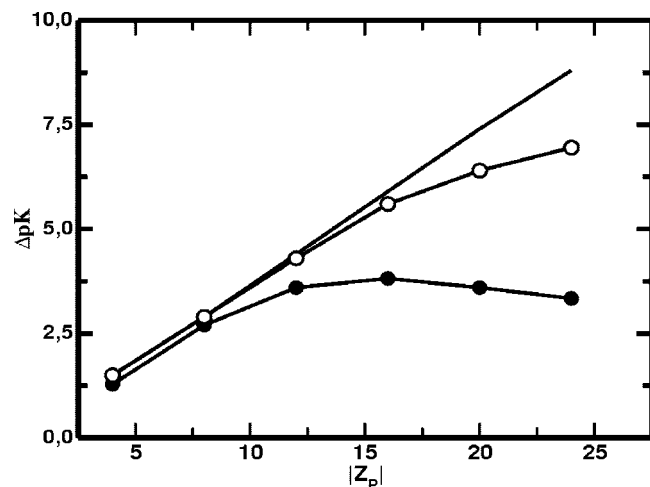


**Figure 3.** The pK shifts as a function of the macromolecular net charge number. Salt concentration is changed from  $C_s = 1$  mM (reference state) to  $C_s = 100$  mM. Results from MC simulations are obtained considering  $R_c = 270.63$  Å ( $C_p = 0.02$  mM) and shown with filled circles. Solid lines without symbols and with open circles denote the linear (DH/LPB) and nonlinear (NLPB) mean field results, respectively. The excess chemical potential for the free ligand contribution ( $\mu_F^{\text{ex}}$ ) on the PB approaches were obtained by eq 12 and assumed  $\kappa^{-1} = \kappa_{\text{DH}}^{-1}$  (see the text for more details). MC errors are estimated to be smaller than 0.1 kT. pK shifts are given in units of kT.

calcium binding shifts) and stability of different proteins has not yet been examined within the context of the PBE approach but one can use the reported experimental data to examine if this is indeed the case.<sup>128,129</sup>

**Poisson–Boltzmann and Monte Carlo Approaches.** The second issue to be discussed here is the comparison between MC and NLPB predictions and the understanding of the physical sources for the found difference in  $\Delta pK$  obtained with the approaches reported above. pK shifts for calcium-binding upon addition of salt obtained by the linear mean field approach and MC simulations at low macromolecular concentrations were previously compared by us.<sup>42</sup> The found disagreement between MC and the PB approaches for sufficiently charged systems ( $Z_p > 12$ ) in principle could be improved by replacing the linearization in the Debye–Hückel equation by a more accurate theory. Nevertheless, as far as we are aware the nonlinear response was not yet tested. Since the description of highly charged aggregates, such as DNA in the presence of multivalent ions, where ion–ion correlations are well known to become more important requires a correlated theory or numerical simulations (Monte Carlo or molecular dynamics),<sup>130,131</sup> it is not possible to be ahead of performing new calculations to predict whether or not the nonlinear PB theory will be sufficient to accurately describe this class of binding phenomena. Therefore, nonlinear PB calculations were carried out as described above in order to provide the pK shifts values for such comparison and analysis. The results are seen in Figure 3. The discrepancy between MC and NLPB starts around  $Z_p = -12$  while no difference is seen between LPB and NLPB at this charge regime. It turns out that increasing the protein net charge makes both LPB and NLPB to overestimate the MC data. The discrepancy between MC and PBE is stronger for the LPB prediction. In this case, the effect of the linearization starts to be significant for  $|Z_p| > 16$  when comparing LPB and NLPB. Indeed, it is well known that NLPB is needed to produce better agreement with the experimental results.<sup>132,133</sup> Figure 3 shows for instance disagreements on the order of ca. 3.5 pK units between the pK shifts obtained through the MC method and

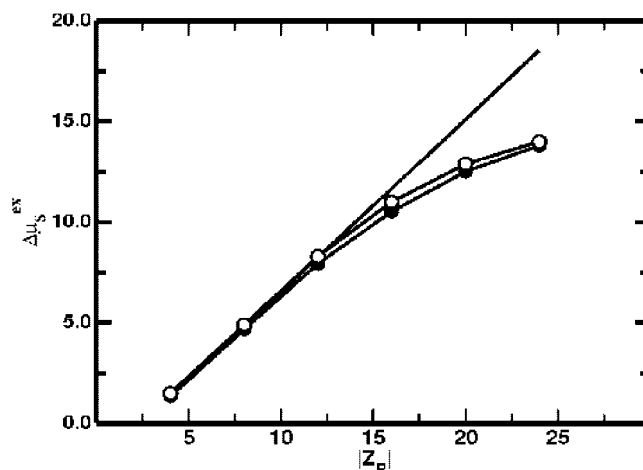


**Figure 4.** The bound component of the binding free energy [ $\Delta\mu_s^{\text{ex}} = \mu_s^{\text{ex}}(C_s = 100 \text{ mM}) - \mu_s^{\text{ex}}(C_{s,\text{ref}} = 1 \text{ mM})$ ] is plotted as a function of the protein net charge number ( $Z_p$ ) at the low macromolecular concentration regime ( $C_p = 0.02$  mM). Reduced excess chemical potentials are given in kT units. All experimental conditions and symbols are the same of Figure 3.

nonlinear mean field approach for a highly charged protein at a high macromolecular concentration. It is important to point out that the final state in this plot is  $C_s = 100$  mM and not  $C_s = 500$  mM, as shown in Figure 2. Despite the differences on the final state, the system qualitative behavior is the same whatever salt concentration ( $C_s > 1$  mM) is chosen to be compared with the reference state.

**Physical Source of the Discrepancy between MC and PBE Predictions.** According to Section II, the electrostatic component of binding free energy is given by a “bound contribution”,  $\mu_s^{\text{ex}} (= G_{\text{holo}}^{\text{el}} - G_{\text{apo}}^{\text{el}})$  and a “free contribution”,  $\mu_F^{\text{ex}}$ . We shall start the analysis with the bound term.

The variation of the bound contribution due the increase on the salt concentration is shown in Figure 4 for a low macromolecular concentration that mimicks the system behavior at an infinite dilution. In this case, Monte Carlo calculations were made with a cell radius  $R_c = 270.63$  Å, which corresponds to a protein concentration  $C_p = 0.02$  mM. At this macromolecular concentration, the protein screening effects are known to be sufficient small.<sup>2,43</sup> A linear dependence between  $\Delta\mu_s^{\text{ex}}$  and  $Z_p$  is observed by the linear mean field approach (equivalent to the TK prescription). This behavior is shared by the nonlinear approach and MC simulations in the low macromolecular charge regime. For macromolecules sufficiently charged the linearization of the Boltzmann term in the PBE causes a disagreement between the results obtained by the linear and the two others approaches. However, the nonlinear mean field and MC simulation results keep good agreement indicating a small effect of ionic correlations in this protein concentration regime. There is just a small tendency for the NLPB to overestimate the MC data. Therefore, we can conclude that the origin of the discrepancy between MC and LPB observed for the bound component  $\mu_s^{\text{ex}}$  in this figure comes from nonlinear thermal effects that were simplified by the TK prescription. From this result, one could have a natural tendency to associate it with the ionic correlation phenomena. As it will be more clearer later, this is not the case, and a perfect agreement between MC and NLPB can be seen if some care is taken (see Section IV).

In order to investigate why such agreement was seen in Figure 4 one needs to analyze the ionic distribution around the charged protein. Figure 5 shows the counterions concentration profiles as a function of the spatial separation distance from the

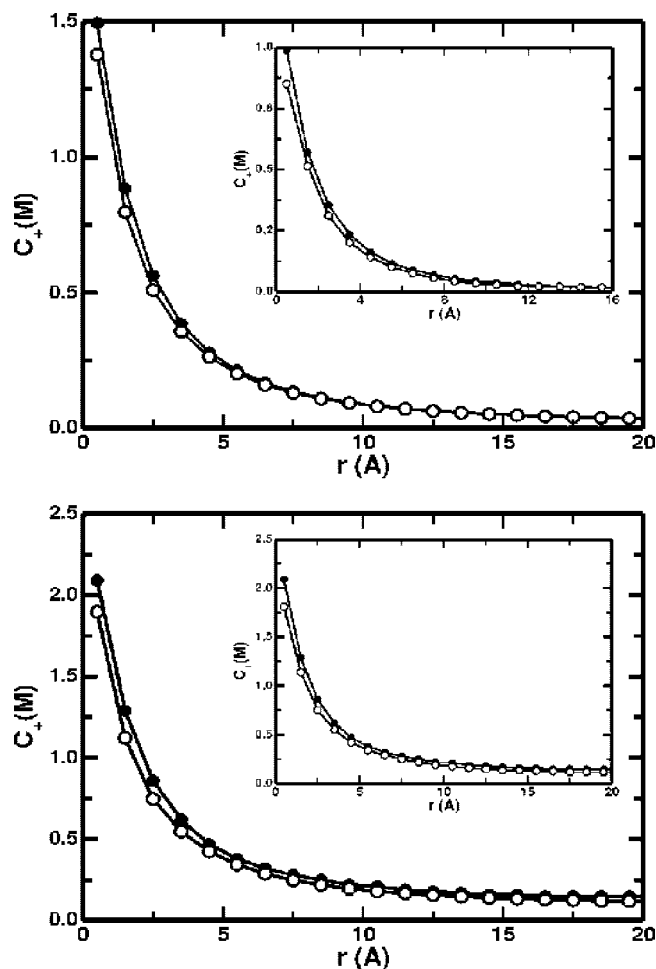


**Figure 5.** Counterions concentration profiles as a function of spatial separation distance from the macromolecule surface for a highly charged protein ( $Q_p = -24e$ ). Results obtained by the PB and the MC simulations are compared as filled and open symbols, respectively. Inner (inserts) and outer graphs correspond to  $C_p = 0.2$  mM and  $C_p = 2$  mM, respectively. The PB data were obtained with the PBCell solver that accounts for macromolecular concentrations (finite macromolecular concentration regime).<sup>125</sup> Top figure: system at low salt concentration ( $C_s = 1$  mM). Bottom figure: system at near physiological ionic strength ( $C_s = 100$  mM).

macromolecular surface ( $R = 0$  Å corresponds to an ion at the contact with the protein surface) at low ( $C_s = 1$  mM) and near physiological ( $C_s = 100$  mM) ionic strengths for two distinct macromolecular concentrations ( $C_p = 0.2$  mM and  $C_p = 2$  mM). These data were sampled for a highly charged spherical macromolecule ( $Q_p = -24e$ ). Similar picture can be seen for the coion distribution profiles. Figure 5a,b illustrated the good agreement between the MC simulation and the nonlinear mean field predictions obtained by a PB solver especially designed to work with the cell model and finite macromolecular concentrations.<sup>125</sup> At the higher salt concentration (see Figure 5b), the macromolecular electrostatic potential is sufficiently screened out already at short separation distances. This means that the Debye screening length at this system condition is much shorter than  $R_c$ . Consequentially,  $R_c$  has virtually no influence on the ionic distribution profile. However, at the low ionic strength regime (see Figure 5a) a decrease of  $R_c$  increases the ionic charge concentration values near the macromolecular surface contact. This is a consequence of the need to satisfy the condition of null electric field in the cell boundary. In practice, what is seen is the increase of the Coulomb shielding as a consequence of the macromolecular concentration which con-

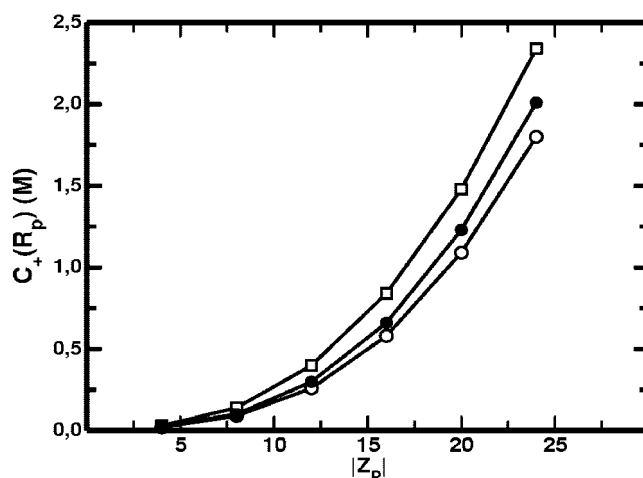


**Figure 6.** Counterions concentration values at the macromolecular surface as a function of the protein net charge number at physiological ionic strength ( $C_s = 100$  mM) and high protein concentration ( $C_p = 2$  mM). The filled and open circles represent the results obtained by the traditional PB solution with cell model and the MC method. The open square denotes results obtained by the modified PBE (MNLBP as given by eq 10).

firms the experimental and theoretical results demonstrated by Linse and co-workers.<sup>2,25</sup> By this comparison, one can verify that the ion–ion correlation effects are of minor importance in the determination of the ionic concentration profiles at this particular (weak) coupling regime<sup>44–46</sup> as it might be expected. In a practical view, the protein screening effect gives an effective macromolecular surface charge density ( $\sigma_{s,eff}$ ) that is smaller than the less screened case ( $\sigma_{s,eff} < \sigma_s$ ) which means that  $\Xi(\sigma_{s,eff})$  at higher macromolecular concentrations is also smaller than  $\Xi(\sigma_s)$  in a more diluted solution [ $\Xi(\sigma_{s,eff}) < \Xi(\sigma_s)$ ]. Small deviations on the ionic profile at short separation distances must not have considerable effects for the  $\Delta\mu_s^x$ , since  $G_{holo}^{el}$  and  $G_{apo}^{el}$  depend on the integration over the whole cell volume. Therefore, according to Figure 4, the utilization of the PB equation and the cell model should efficiently describe  $\Delta\mu_s^x$  at all these protein and salt concentrations conditions.

For the regimes considered here, the electrostatic screening will be at its maximum at high protein concentration and physiological ionic strength. This is also where  $\Xi$  will have the smallest value. The counterion concentration values at the macromolecular surface contact as a function of the protein net charge at this situation ( $C_s = 100$  mM and  $C_p = 2$  mM) are shown in Figure 6. The good agreement between the results obtained by the MC and the nonlinear approach of PB reproduces the behavior of Figure 5. As it is expected, increasing the electrostatic coupling (i.e., here the protein net charge, or, equivalently, the macromolecular surface charge density  $\sigma_s$ )<sup>44–46</sup> gives rise to more pronounceable differences between PB and MC, although on all range of protein charges analyzed by the MC calculations give only slightly larger values for the counterion concentrations at the contact region. This observation might be attributed to small ionic correlation effects (principally due the finite particle size neglected when PB treats free mobile ions as point particles). The results obtained by the modified PBE as suggested by eq 10 (MNLBP) are also shown in this plot. The introduction of the third term,  $(|Q_p|/e)C_p \exp(-\beta\phi)$ , in eq 10 overestimates the counterion concentration values in relation to the other two approaches. At the physiological salt concentration condition, the higher macromolecular concentration shown here is the most critical case in our present study for the protein screening phenomena. It is well known that the



**TABLE 1: The Differences between the Excess Chemical Potential of a Divalent Ion in an Electrolyte Solution (1:1) in the Presence of a Charged Macromolecule ( $\mu_F^{\text{ex}}$ ) and in a Bulk Electrolyte Solution ( $\mu_{\text{bulk}}^{\text{ex}}$ )<sup>a</sup>**

$Z_p$	macromolecular concentration			
	$C_p = 0.02 \text{ mM}$		$C_p = 2 \text{ mM}$	
	$\Delta\mu_F^{\text{ex}}$	$\Delta\mu_{F,\text{solution}}^{\text{ex}}$	$\Delta\mu_F^{\text{ex}}$	$\Delta\mu_{F,\text{solution}}^{\text{ex}}$
-4	-0.195	0.130	-0.676	0.836
-8	-0.313	0.399	-1.186	2.054
-12	-0.619	0.677	-1.886	3.261
-16	-1.100	0.952	-2.637	4.429
-20	-1.307	1.225	-3.751	5.596
-24	-1.643	1.500	-4.261	6.745

<sup>a</sup> Data from MC runs with the cell model. The terms  $\Delta\mu_F^{\text{ex}} (= \mu_F^{\text{ex}} - \mu_{\text{bulk}}^{\text{ex}})$  and  $\Delta\mu_{F,\text{solution}}^{\text{ex}} (= \mu_{F,\text{solution}}^{\text{ex}} - \mu_{\text{bulk}}^{\text{ex}})$  refer to the total excess chemical potential and the chemical potential contribution term due the electrolyte solution only (here, the ligand-macromolecule interaction is excluded), respectively. Charges are given in  $e$ , and the chemical potentials in kT. In all cases, the relative permittivity of the solvent region is  $\epsilon_s = 78.7$ . Standard deviations were obtained by block subaveraging over the production runs and estimated to be less than 0.02.

PB approach is rendered useless by the increase of electrostatic coupling (e.g., increasing  $Z_p$ ).<sup>40,44–46</sup> However, the differences for the counterion concentration values at the macromolecular contact for the highly charged protein (the most critical one in the present study) between the MC and modified PB data, and the MC and the standard PB outcomes is 0.33 and 0.21 M, respectively. For higher ionic strengths, this discrepancy should decrease due to the reduction of the ratio  $(|Z_p|C_p/C_s)$ . We can speculate here that since MC and traditional PB have such good agreement on  $\Delta\mu_F^{\text{ex}}$ , any disagreement on  $\Delta pK$ s must have the  $\Delta\mu_F^{\text{ex}}$  contribution as the main origin. Indeed, this will be shown to be the case.

As mentioned above, in the hypothetical experimental situation of null macromolecular concentration, the binding free energy is the isothermal work needed to bring a ligand located from a position far away of the macromolecule, where the solution recovers its bulk characteristics to its binding site position. Therefore, the use of the relation 12 to calculate  $\mu_F^{\text{ex}}$  is a reasonable choice (valid for  $C_p \rightarrow 0$ ). However, in a finite macromolecular concentration ( $C_p \gg 0$ ), two other contributions should also be considered: (a) the interaction between the charged macromolecule and the ligand, and (b) the heterogeneity of the electrolyte solution modified by the presence of such highly charged object. Both  $\Delta\mu_F^{\text{ex}}$  and  $\Delta\mu_{F,\text{solution}}^{\text{ex}}$  are affected by these contributions.

Table 1 presents the excess chemical potential differences for a divalent ligand in a symmetrical 1:1 electrolyte solution obtained by MC simulation at two different macromolecular concentrations and in a low ionic strength condition. The component due to the electrolyte solution, excluding the electrostatic interaction ligand–macromolecule, is shown as well. Note however that this term reflects the arrangement (packing) of the free ions due the macromolecular charge. Only the static electrostatic contribution was subtracted off. It can be observed that even for a weak protein net charge,  $\mu_F^{\text{ex}}$  is affected by the protein concentration, since all free charged species in the solution interact with the macromolecular charge. For instance, the redistribution of charges around the central macroion affects  $\mu_{F,\text{solution}}^{\text{ex}}$  by a factor of 8 for  $Z_p = -4$ , when comparing  $\Delta\mu_{F,\text{solution}}^{\text{ex}}$  at  $C_p = 0.02 \text{ mM}$  and  $C_p = 2 \text{ mM}$ . The ionic distribution profiles indicate the same trends as seen above. Moreover, in a 1:1 electrolyte solution the divalent charged

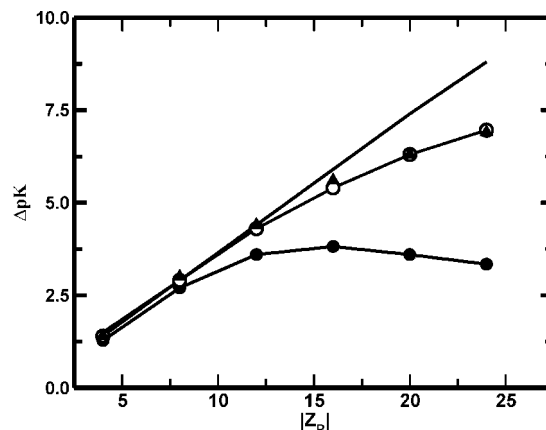


**Figure 7.** The pK shifts as a function of the macromolecular net charge. Results from MC simulations where  $\mu_F^{\text{ex}}$  is obtained in a simulation cell in the absence of the charged macromolecule (its bulk value) are represented by the filled triangles. All the other details are the same as Figure 3.

ligand interacts with the macromolecule stronger than any other charged specie. The effect of the macromolecular charge dominates the excess term of the ligand chemical potential. This phenomena is enlarged at high macromolecular concentration and as a consequence is responsible for the discrepancy observed in Figure 3. Qualitatively, the situation is the same even for stronger ionic strengths. At  $C_s = 100 \text{ mM}$  and  $C_p = 2 \text{ mM}$ ,  $\Delta\mu_{F,\text{solution}}^{\text{ex}}$  varies from 0.243 for  $Z_p = -4$  to 6.201 for  $Z_p = -24$ .

To confirm that the found discrepancy between MC and NLPB data for the salt pK shifts calculations are solely due a inconsistent manner that  $\mu_F^{\text{ex}}$  is usually treated in this kind of study, we have measured  $\mu_F^{\text{ex}}$  by the insertions of the (virtual) ligand particle in random position within a separated bulk simulation cell (in the absence of the charged macromolecule). Doing that,  $\mu_F^{\text{ex}}$  is obtained under the same experimental conditions by all the three approaches (MC, LPB, and NLPB), that is, at the infinite macromolecular dilution regime. As can be seen in Figure 7, if the protein concentration effect is not taken into account when measuring  $\mu_F^{\text{ex}}$ , MC data recover the NLPB results. Alternatively,  $\mu_F^{\text{ex}}$  on the PB approaches could be obtained by eq 11 assuming  $\kappa_{BS}^{-1}$  instead of  $\kappa_{DH}^{-1}$ . This means that the replacement of the linear by the nonlinear thermal response is enough to result in equally well numbers when comparing numerical calculations (PB) with simulations (MC). In other words, the initial observed discrepancy (see Figure 3) is not related with ion–ion correlations as it could be argued. Moreover, the linear approach does a good job for even more relatively higher charged proteins than supposed before.<sup>42</sup> This plot also provides a practical view to decide which protocol one should use for each protein charge system. The effect of the nonlinear thermal response becomes very significant when  $Z_p$  is increased to values larger than 15. Of course, in order to correctly incorporate the macromolecular screening into the calculations one has to either adopt a modified  $\kappa$  (e.g.,  $\kappa_{BS}^{-1}$ ) on the PB solvers or obtain  $\mu_F^{\text{ex}}$  by the insertions of Widom particles in the presence of the charged macromolecule as we did for the data reported in Figure 3.

## V. Concluding Remarks

Monte Carlo simulations and Poisson–Boltzmann approaches associated with the assumption of a mean field description were used to analyze binding constants at different experimental

conditions providing a physical interpretation for the found agreements and discrepancies. Invoking a PB solver that takes into account the macromolecular volume fraction (cell model), we have demonstrated that ionic concentration distribution profiles predicted by PB and MC are in good agreement for the systems here studied and the experimental conditions used in this work. These findings show that ionic correlation effects are of minor importance at the experimental conditions described here with symmetrical 1:1 electrolyte solutions. By the comparison of  $pK$  shifts upon addition of salt predicted by the different theoretical schemes, it can be concluded that the main reason that makes the PB theory “less” reliable in such applications is simply due the manner in which it approximates the excess chemical potential of the ligand (using its value in the corresponding bulk salt solution). The observed failure may not be attributed to the use of linear or nonlinear thermal treatments (DH/LPB versus NLPB) and/or explicit ion–ion interactions as initially believed. In fact, since ion–ion correlations were apparently the best explanation in principle to justify the observed physical mechanism, this result gains importance offering an alternative interpretation and a simple practical procedure to improve PB calculations.

Our findings also show that the nonlinear PB predictions with a low dielectric response reproduce well the calculations with the homogeneous dielectric model. This is an important result in order to provide a more solid basis on the intense and controversial debate about the protein dielectric modeling. From our present data, one can see that a uniform dielectric permittivity can be assigned for the whole system for simplified models such as the one used here. Being in principle that the dielectric constant is a macroscopic physical property, this seems to be a reasonable choice principally when one has to handle atomic charges that can be at relatively short distances ( $<5 \text{ \AA}$ ) where the macroscopic idea loses its real meaning. The reduction in the computational costs in a numerical simulation when replacing the dielectric interface by a uniform dielectric constant used to the whole system is substantially and surely appealing. However, additional experimental and theoretical studies are required in order to assess the ability of the different theoretical models and solutions such as Poisson–Boltzmann, Monte Carlo, and Tanford–Kirkwood in accurately capturing the salt dependence of different equilibria processes such the ionization of biomolecules. Thus, any conclusions about the electrostatic binding free energy should be made with caution keeping in mind the model and the solvers’ approximations, especially when inferring if the electrostatic contribution to the binding is favorable or unfavorable for a particular ligand–receptor system being treated.

**Acknowledgment.** This work has been supported in part by the Conselho Nacional de Desenvolvimento Científico e Tecnológico (CNPq) and Fundação de Amparo à Pesquisa do Estado de São Paulo (Fapesp) whom we (F.L.B.D.S. and S.J.C.) wish to thank. One of us (M.O.F.) would like to thank the NSF-CHEM-0137961 for support during this collaborative project. It is also a pleasure to acknowledge fruitful discussions with Bo Jönsson, João Ruggiero Neto, and Maarten Biesheuvel and their insightful comments. The DelPhi calculations were possible due to a kind license offered by Honig’s laboratory. The PBCell solver was kindly provided and explained by Bengt Jönsson whom we also have the pleasure to acknowledge. The suggestions of anonymous referees were greatly appreciated too.

## References and Notes

- (1) Bamborough, P.; Cohen, F. E. *Curr. Opin. Struct. Biol.* **1996**, *6*, 236.
- (2) da Silva, F. L. B.; Linse, S.; Jönsson, B. *J. Phys. Chem. B* **2005**, *109*, 2007.
- (3) Lund, M.; Jönsson, B. *Biophys. J.* **2003**, *85*, 2940.
- (4) Archontis, G.; Simonson, T. *Biophys. J.* **2005**, *88*, 3888.
- (5) de Kruif, C. G.; Weinbreck, F.; de Vries, R. *Curr. Opin. Colloid Interface Sci.* **2004**, *9*, 340.
- (6) Gilson, M. K.; Honig, B. *Nature* **1987**, *330*, 84.
- (7) Sternberg, M. J. E.; Hayes, F. R. F.; Russell, A. J.; Thomas, P. G.; Fersht, A. R. *Nature* **1997**, *330*, 86.
- (8) Sheinerman, F. B.; Honig, B. *J. Mol. Biol.* **2002**, *318*, 161.
- (9) Zhou, H.-X.; Wong, K.-Y.; Vijayakumar, M. *Proc. Natl. Acad. Sci. U.S.A.* **1997**, *94*, 12372.
- (10) Broijmans, N.; Kuntz, I. D. *Annu. Rev. Biophys. Biomol. Struct.* **2003**, *32*, 335.
- (11) Evenäs, J.; Malmendal, A.; Forsén, S. *Curr. Opin. Struct. Biol.* **1998**, *2*, 293.
- (12) M-Bentley, A.; Réty, S. *Curr. Opin. Struct. Biol.* **2000**, *10*, 637.
- (13) Hubbell, J. A. *Science* **2003**, *300*, 595.
- (14) Warshel, A. *Annu. Rev. Biophys. Biomol. Struct.* **2003**, *32*, 425.
- (15) da Silva, F. L. B.; Lund, M.; Jönsson, B.; Åkesson, T. *J. Phys. Chem. B* **2006**, *110*, 4459.
- (16) Kirkwood, J. G. *J. Chem. Phys.* **1934**, *2*, 351.
- (17) Madura, J. D.; et al. In *Reviews in Computational Chemistry*; Lipkowitz, K. B., Boyd, D. B., Eds.; VCH Publishers, Inc.: New York, 1994; Vol. 5, pp 229–267.
- (18) Jönsson, B.; Svensson, B. In *Computer Simulation of Biomolecular Systems*; van Gunsteren, W. F., Weiner, P. K., Wilkinson, A., Eds.; ESCOM: Leiden, The Netherlands, 1993; Vol. 2, pp 464–482.
- (19) Bashford, D.; Karplus, M. *Biochemistry* **1990**, *29*, 10219.
- (20) Bashford, D.; Gerwert, K. *J. Mol. Biol.* **1992**, *224*, 473.
- (21) Holst, M.; Baker, N.; Wang, F. J. *Comput. Chem.* **2000**, *21*, 1319.
- (22) Warshel, A.; Papazyan, A. *Curr. Opin. Struct. Biol.* **1998**, *8*, 211.
- (23) Boschitsch, A. H.; Fenley, M. O. *J. Comput. Chem.* **2004**, *25*, 935.
- (24) Kesvatera, T.; Jönsson, B.; Thulin, E.; Linse, S. *Biochemistry* **1996**, *33*, 14170.
- (25) Linse, S.; Jönsson, B.; Chazin, W. J. *Proc. Natl. Acad. Sci. U.S.A.* **1995**, *92*, 4748.
- (26) Linderström-Lang, K. C. R. *Trav. Lab. Carlsberg* **1924**, *15*, 1.
- (27) Tanford, C.; Kirkwood, J. G. *J. Am. Chem. Soc.* **1957**, *79*, 5333.
- (28) Friedman, H. L. *Annu. Rev. Phys. Chem.* **1981**, *32*, 179.
- (29) Jorgensen, W. L.; Chandrasekhar, J.; Madura, J. D.; Impey, R. W.; Klein, M. L. *J. Chem. Phys.* **1983**, *79*, 926.
- (30) Sham, Y. Y.; Chu, Z. T.; Warshel, A. *J. Phys. Chem. B* **1997**, *101*, 4458.
- (31) Stigter, D.; Dill, K. A. *Biochemistry* **1990**, *29*, 1262.
- (32) van Gunsteren, W. F.; Berendsen, H. J. C. *Angew. Chem., Int. Ed. Engl.* **1990**, *29*, 992.
- (33) Jorgensen, W. L.; Maxwell, D. S.; Tirado-Rives, J. *J. Am. Chem. Soc.* **1996**, *118*, 11225.
- (34) Rocchia, W.; Alexov, E.; Honig, B. *J. Phys. Chem.* **2001**, *105*, 6507.
- (35) Warshel, A.; Åqvist, J. *Annu. Rev. Biophys. Biomol. Struct.* **1991**, *20*, 267.
- (36) Jönsson, B.; Lund, M.; da Silva, F. L. B. In *Food Colloids: Self-Assembly and Material Science*; Dickinson, E., Leser, M. E., Eds.; Royal Society of Chemistry: London, 2007; pp 129–154.
- (37) Warwicker, J.; Watson, H. C. *J. Mol. Biol.* **1982**, *157*, 671.
- (38) Fogolari, F.; Brigo, A.; Molinari, H. J. *Mol. Recog.* **2002**, *15*, 377.
- (39) Borkovec, M.; Jönsson, B.; Koper, G. J. M. *Ionization Processes and Proton Binding in Polyprotic Systems: Small Molecules, Proteins, Interfaces and Polyelectrolytes*; Leiden University: Leiden, The Netherlands, 1999.
- (40) Jönsson, B.; Åkesson, T.; Woodward, C. In *Ordering and phase transitions in charged colloids*; Arora, A. K., Tata, B. V. R., Eds.; VCH: New York, 1996; pp 295–313.
- (41) Degreuve, L.; Lozada-Cassou, M. *Mol. Phys.* **1995**, *86*, 759.
- (42) da Silva, F. L. B.; Jönsson, B.; Penfold, R. *Protein Sci.* **2001**, *10*, 1415.
- (43) de Carvalho, S. J.; Ghiotto, R. T.; da Silva, F. L. B. *J. Phys. Chem. B* **2006**, *110*, 8832.
- (44) Netz, R. R. *Eur. Phys. J. E* **2001**, *5*, 557.
- (45) Naji, A.; Arnold, A.; Holm, C.; Netz, R. R. *Eur. Phys. J. E* **2001**, *5*, 557.
- (46) Linse, P. *Adv. Polym. Sci.* **2005**, *185*, 111.
- (47) Fushiki, M.; Svensson, B.; Jönsson, B.; Woodward, C. E. *Biopolymers* **1991**, *31*, 1149.
- (48) Degreuve, L.; Lozada-Cassou, M.; Sánchez, E.; Gonzáles-Tovar, E. *J. Chem. Phys.* **1993**, *98*, 8905.

- (49) Hribar, B.; Vlachy, V. *Biophys. J.* **2000**, *78*, 694.
- (50) Guldbrand, L.; Jönsson, B.; Wennerström, H.; Linse, P. *J. Chem. Phys.* **1984**, *80*, 2221.
- (51) Quesada-Pérez, M.; González-Tovar, E.; Martín-Molina, A.; Lozada-Cassou, M.; Hidalgo-Álvarez, R. *ChemPhysChem* **2003**, *4*, 234.
- (52) Lin, S.-C.; Lee, W. I.; Shurr, J. M. *Biopolymers* **1978**, *17*, 1041.
- (53) *Macro-ion Characterization: From Dilute Solutions to Complex Fluids*; Schmitz, K. S., Ed.; American Chemistry Society: Washington, DC; 1994.
- (54) Beresford-Smith, B.; Chan, D. Y. C. *Faraday Discuss. Chem. Soc.* **1983**, *76*, 65.
- (55) Svensson, B.; Jönsson, B.; Thulin, E.; Woodward, C. *Biochemistry* **1993**, *32*, 2828.
- (56) Lodish, H.; Berk, A.; Zipursky, S. L.; Matsudaira, P.; Baltimore, D.; Darnell, J. E. *Molecular Cell Biology*, 4th ed; W. H. Freeman & Company: New York, 1999.
- (57) Wider, G. *BioTechniques* **2000**, *29*, 1278.
- (58) Sader, J. E.; Chan, D. Y. C. *Langmuir* **2000**, *16*, 324.
- (59) Wang, M.; Liu, J.; Chen, S. *Mol. Simul.* **2007**, *33*, 1273.
- (60) Svensson, B.; Jönsson, B.; Woodward, C. E. *Biophys. Chem.* **1990**, *38*, 179.
- (61) Kesvatera, T.; Jönsson, B.; Thulin, E.; Linse, S. *Proteins: Struct., Funct., Genet.* **2001**, *45*, 129.
- (62) Autreto, P. A. S.; Figueiredo, F. V.; Nonato, M. C.; da Silva, F. L. B. *Braz. J. Pharm. Sci.* **2003**, *2*:39, 203.
- (63) Levesque, D.; Weis, J. J.; Hansen, J. P. In *Monte Carlo Methods in Statistical Physics*; Binder, K., Ed.; Springer-Verlag: Berlin, 1986; Vol. 5, pp 47–119.
- (64) Berman, H. M.; Westbrook, J.; Feng, Z.; Gilliland, G.; Bhat, T. N.; Weissig, H.; Shindyalov, I. N.; Bourne, P. E. *Nucleic Acids Res.* **2000**, *28*, 235.
- (65) Protein data bank. <http://www.rcsb.org/pdb> (accessed 2005).
- (66) Iversen, G.; Kharkats, Y. I.; Ulstrup, J. *Mol. Phys.* **1998**, *94*, 297.
- (67) Szebenyi, D. M. E.; Moffat, K. J. *Biol. Chem.* **1986**, *261*, 8761.
- (68) Linse, S.; Brodin, P.; Johansson, C.; Thulin, E.; Grundström, T.; Forsen, S. *Nature* **1988**, *335*, 651.
- (69) Demchuk, E.; Wade, R. C. *J. Phys. Chem. B* **1996**, *100*, 17373.
- (70) Penfold, R.; Warwicker, J.; Jönsson, B. *J. Phys. Chem. B* **1998**, *102*, 8599.
- (71) King, G.; Lee, F. S.; Warshel, A. J. *Chem. Phys.* **1991**, *95*, 4366.
- (72) Antonsiewicz, J.; McCammon, J. A.; Gilson, M. K. *J. Mol. Biol.* **1994**, *238*, 415.
- (73) Simonson, T.; Perahia, D. J. *Am. Chem. Soc.* **1995**, *117*, 7987.
- (74) Simonson, T.; Brooks, C. L., III *J. Am. Chem. Soc.* **1996**, *118*, 8452.
- (75) Antonsiewicz, J.; McCammon, J. A.; Gilson, M. K. *Biochemistry* **1996**, *35*, 7819.
- (76) Löffler, G.; Sreiber, H.; Steinhauser, O. *J. Mol. Biol.* **1997**, *270*, 520.
- (77) Warwicker, J. *Protein Sci.* **1999**, *8*, 418.
- (78) Schutz, C. N.; Warshel, A. *Proteins: Struct., Funct., Genet.* **2001**, *44*, 400.
- (79) Dudev, T.; Lim, C. J. *Phys. Chem. B* **2000**, *104*, 3692.
- (80) Varma, S.; Jakobsson, E. *Biophys. J.* **2004**, *86*, 690.
- (81) He, Y.; Xu, J.; Pan, X.-M. *Proteins: Struct., Funct., Bioinf.* **2007**, *69*, 75.
- (82) Zhou, H. X.; Dong, F. *Biophys. J.* **2003**, *84*, 2216.
- (83) Juffer, A. H.; Vogel, H. J. *Proteins* **2000**, *41*, 554.
- (84) Hingerty, B. E.; Ritchie, R. H.; Ferrell, T. L.; Turner, J. E. *Biopolymers* **1985**, *24*, 427.
- (85) Wisz, M. S.; Hellinga, H. W. *Proteins* **2003**, *51*, 360.
- (86) Morreale, A.; Gil-Redondo, R.; Ortiz, A. R. *Proteins: Struct., Funct., Bioinf.* **2007**, *67*, 606.
- (87) Sharp, K. A.; Nicholls, A.; Sridharan, S. *Delphi - A Macromolecular Electrostatics Modeling Package*; Columbia University: New York, 1998.
- (88) Juffer, A. H. *Biochem. Cell Biol.* **1998**, *76*, 198.
- (89) Svensson, B.; Jönsson, B.; Woodward, C. E.; Linse, S. *Biochemistry* **1991**, *30*, 5209.
- (90) de Vries, R. J. *Chem. Phys.* **2004**, *120*, 3475.
- (91) Carlsson, F.; Linse, P.; Malmsten, M. *J. Chem. Phys.* **2001**, *113*, 4359.
- (92) André, I.; Kesvatera, T.; Jönsson, B.; Åerfeldt, K. S.; Linse, S. *Biophys. J.* **2004**, *87*, 1929.
- (93) Lund, M.; Jönsson, B. *Biochemistry* **2005**, *44*, 5722.
- (94) Biesheuvel, P. M.; Wittemann, A. *J. Phys. Chem. B* **2005**, *109*, 4209.
- (95) de Leeuw, S. W.; Perram, J. W.; Smith, E. R. *Proc. R. Soc. London, Ser. A* **1980**, *373*, 27.
- (96) Metropolis, N. A.; Rosenbluth, A. W.; Rosenbluth, M. N.; Teller, A.; Teller, E. *J. Chem. Phys.* **1953**, *21*, 1087.
- (97) Frenkel, D.; Smit, B. *Understanding Molecular Simulation: From Algorithms to Applications*; Academic Press: San Diego, 1996.
- (98) Svensson, B. R.; Woodward, C. E. *Mol. Phys.* **1988**, *64*, 247.
- (99) Sloth, P.; Sørensen, T. S. *Chem. Phys. Lett.* **1990**, *173*, 51.
- (100) Widom, B. *J. Chem. Phys.* **1963**, *39*, 2808.
- (101) Svensson, B.; Jönsson, B.; Fushiki, M.; Linse, S. *J. Phys. Chem.* **1992**, *96*, 3135.
- (102) McQuarrie, D. A. *Statistical Mechanics*; Harper Collins, New York, 1976).
- (103) Evans, D. F.; Wennerström, H. *The Colloidal Domain*; VCH Publishers, New York, 1994.
- (104) Jönsson, B.; Lindman, B.; Holmberg, K.; Kronberg, B. *Surfactants and Polymers in Aqueous Solution*; John Wiley: Chichester, 1998.
- (105) Jackson, J. *Classical Electrodynamics*; J. Wiley: New York, 1967.
- (106) Böttcher, C. J. F. *Theory of Electric Polarization*; Elsevier: Amsterdam, 1973.
- (107) Hill, T. L. *Statistical Mechanics*; McGraw-Hill: New York, 1956.
- (108) Russel, W. B.; Saville, D. A.; Schowalter, W. R. *Colloidal Dispersions*; Cambridge University Press: Cambridge, 1989.
- (109) Hill, T. L. *An Introduction to Statistical Thermodynamics*; Dover Publications Inc.: New York, 1986.
- (110) Lyklema, J. *Fundamentals of Interface and Colloid Science*; Academic Press: San Diego, 1991.
- (111) Evans, D. F.; Wennerström, H. *The Colloidal Domain where Physics, Chemistry, Technology and Biology meet*; VCH Publishers Inc.: New York, 1994.
- (112) Usui, S. In *Electrical Phenomena at Interfaces—Fundamentals, Measurements, and Applications*; Kitahara, A., Watanabe, A., Eds.; Marcel Dekker, Inc.: New York, 1984, pp 15–46.
- (113) da Silva, F. L. B.; Lund, M.; Jönsson, B.; Åkesson, T. *J. Phys. Chem. B* **2006**, *110*, 4459.
- (114) Davis, M. E.; McCammon, J. A. *Chem. Rev.* **1990**, *90*, 509.
- (115) Project, C. S. E. *Direct and Inverse Bioelectric Field Problem*. <http://csep1.phy.ornl.gov/bf/bf.html> (accessed 1995).
- (116) Harvey, S. C. *Proteins: Struct., Funct., Genet.* **1989**, *5*, 78.
- (117) Ortung, W. H. *Ann. N.Y. Acad. Sci.* **1977**, *303*, 22.
- (118) Holst, M. Ph.D. Thesis, University of Illinois at Urbana-Champaign, Urbana, IL, 1993.
- (119) Davis, M. E.; Madura, J. D.; Luty, B. A.; McCammon, J. A. *Comput. Phys. Commun.* **1991**, *62*, 187.
- (120) Juffer, A. H. Ph.D. Thesis, Rijksuniversiteit Groningen, The Netherlands, 1993.
- (121) Jufer, A. H.; Botta, E. F. F.; van Keulen, B. A. M.; van der Ploeg, A.; Berendsen, H. J. C. *J. Comp. Phys.* **1991**, *97*, 144.
- (122) Boschitsch, A. H.; Fenley, M. O.; Zhou, H. X. *J. Phys. Chem. B* **2002**, *106*, 2741.
- (123) Honig, B.; Nicholls, A. *Science* **1995**, *268*, 1144.
- (124) Juffer, A. H. *Melc—The Macromolecular Electrostatics Computer program*; Laboratory of Physical Chemistry: University of Groningen, The Netherlands, 1992.
- (125) Jönsson, B. Ph.D. Thesis, Lund University, Lund, Sweden, 1981.
- (126) Baker, N. A.; Sept, D.; Joseph, S.; Holst, M. J.; McCammon, J. A. *Proc. Natl. Acad. Sci. U.S.A.* **2001**, *98*, 10037.
- (127) Beresford-Smith, B. Ph.D. Thesis, Australian National University, Canberra, Australia, 1985.
- (128) Kao, Y.-H.; Fitch, C. A.; Bhattacharya, S.; Sarkisian, C. J.; Lecomte, J. T. J.; Garcia-Moreno, B. *Biophys. J.* **2000**, *79*, 1637.
- (129) Wunderlich, M.; Martin, A.; Schmid, F. X. *J. Mol. Biol.* **2005**, *347*, 1063.
- (130) Guldbrand, L.; Nilsson, L.; Nordenskiöld, L. *J. Chem. Phys.* **1986**, *85*, 6686.
- (131) Mel'nikov, S.; Lindman, B.; Khan, M. O.; Jönsson, B. *J. Am. Chem. Soc.* **1999**, *121*, 1130.
- (132) Hecht, J. L.; Honig, B.; Shin, Y. K.; Hubbell, W. L. *J. Phys. Chem.* **1995**, *99*, 7782.
- (133) Bertonati, C.; Honig, B.; Alexov, E. *Biophys. J.* **2007**, *92*, 1891.